PHYSICAL REVIEW C VOLUME 24, NUMBER 6 DECEMBER 1981

Distorted wave impulse approximation calculations of $(\pi^+,2p)$ reactions in a quasideuteron model

P. G. Roos, L. Rees, and N. S. Chant
Department of Physics and Astronomy, University of Maryland, College Park, Maryland 20742
(Received 20 July 1981)

A formalism for distorted wave impulse approximation calculations of the $A(\pi^+,2p)B$ reaction to discrete states in nucleus B is described. Assuming that the π^+ capture occurs on a deuteronlike structure in the target nucleus, calculations are presented covering a range of bombarding energies from 25 to 350 MeV and target nuclei from $A=16$ to 90. In most cases, distortion effects arising from the interaction of the pion and two outgoing protons with the core are large, but primarily affect the magnitude of the cross section. Based on these calculations it is concluded that any more realistic calculation of pion absorption will require the inclusion of the interaction of the incoming and outgoing particles with the core.

[NUCLEAR REACTIONS DWIA reaction theory of pion absorption on nuclei. ^{16}O, ^{40}Ca, ^{90}Zr$(\pi^+,2p)$, $T_\pi=25-350$ MeV, calculate $\sigma(\theta_1,\theta_2,E_1)$.]

I. INTRODUCTION

The pi-meson capture process (π,NN) has long been considered an important reaction to examine and understand. One reason for its importance is that at low pion energies it is the dominant component of the reaction cross section, and is thus an essential ingredient to an understanding of pi-nucleus interactions. In a more speculative vein, the reaction has often been proposed as a source of information on short-range correlations in nuclei, since the two nucleons are released with rather large relative momentum ($\gtrsim 0.8$ GeV/c).

Unfortunately, in spite of interest in this reaction, there exists so far rather little experimental data appropriate for direct comparisons with theory. This situation arises primarily from the lack, until recently, of high quality pion beams, the rather small cross section for the reaction, and the necessity of detecting relatively high energy nucleons, thereby leading to poor energy resolution.

Much of the existing data have been taken with stopped π^- beams. However, in recent years the situation has improved somewhat with the availability of more extensive, higher resolution, in-flight capture experiments, as well as $(\pi^-,2n)$ experiments with stopped π^- beams. Favier *et al.*[1] have studied the $(\pi^+,2p)$ reaction at 76 MeV on a series of nuclei ranging from He to Pb. The resultant missing energy resolution was approximately 6 MeV. Arthur *et al.*[2] have also studied the $(\pi^+,2p)$ reaction at 70 MeV on ^{6}Li, ^{14}N, and ^{16}O with a missing energy resolution of 4.5 MeV. Bassalleck *et al.*[3] and Ullrich[4] have examined the $(\pi^-,2n)$ reaction on a series of light nuclei with stopped π^- particles. These experiments provided a missing energy resolution of order 3–6 MeV. In all three experiments the energy resolution was insufficient to cleanly separate nuclear states, except in the case of ^{6}Li. In addition, in order to obtain adequate statistics, these papers reported results as a function of recoil momentum for very large effective solid angles. Thus, comparison with theory is difficult without detailed knowledge of the specific detector geometries and a tedious folding calculation. Nevertheless, the extensive investigations of these experiments in fact provide a great deal of guidance in the theoretical treatment, as will be discussed.

Various theoretical calculations[5–13] of the

 ©1981 The American Physical Society

(π,NN) process have been carried out with, at best, modest success. Most of the emphasis has been on the $\pi(NN)$ vertex. However, it has proven difficult to obtain a satisfactory description of the $\pi^+ + d \rightarrow 2p$ two-body reaction (e.g., see Refs. 5 and 6), and applications to heavier nuclei have been discouraged. The existing calculations generally concentrate on pionic atoms and have included a myriad of terms associated with the $\pi(NN)$ vertex, such as initial state pion rescattering, short-range correlations, D-state contributions, and final state nucleon-nucleon interactions (e.g., see Refs. 7—13 and references therein). Probably the most recent detailed work on capture in pionic atoms is that of Shimizu and Faessler[13] which examines the contributions from the various terms mentioned above, as well as intermediate Δ production.

While much effort has been expended in calculations of the $\pi(NN)$ vertex, rather little work has been reported on the treatment of the interactions of the projectile and outgoing nucleons with the residual nucleus. Studies of the mass dependence of the $(\pi^+,2p)$ reaction by Favier *et al.*[1] show that the cross section depends on target mass as $A^{0.4}$, suggesting strong localization of the reaction to the nuclear surface and thereby the importance of the interactions with the residual nucleus. Calculations which do include the nucleon-nucleus final state interaction are those of Garciliazo and Eisenberg[12] and Shimizu and Faessler,[13] also reported in Ref. 4. However, in these calculations the final state distortion is included in an approximate manner, and its importance is indicated but not separately delineated. Thus, both the experimental and theoretical results indicate a need to include distortions due to the residual nucleus on an equal basis with the $\pi(NN)$ vertex, at least if one hopes to extract quantitative information from the (π,NN) reaction.

In our present calculations, we have attempted a quantitative investigation of effects due to interactions with the residual nucleus. Since the role of distortion effects in the (π,NN) reaction has generally been neglected one needs to evaluate their importance at various energies and for various target masses. To this end we utilize a distorted wave impulse approximation (DWIA) formulation in which we assume the pion capture takes place on a deuteronlike component of the target nucleus wave function, and the $\pi(NN)$ vertex is then obtained using the impulse approximation.

The use of a quasideuteron DWIA model is primarily motivated by the necessity of reducing this complex reaction to a practical calculation. The model allows us to examine in detail the effects and importance of distortion arising from interactions with the core. In addition, there is experimental and theoretical support for the use of this model.

(1) A study of the angular dependence of the $(\pi^+,2p)$ reaction on light nuclei[2] shows remarkably good agreement with the angular dependence of the $\pi^+ + d \rightarrow 2p$ two-body reaction.

(2) Tests of the factorization approximation using the Triemann-Yang angles[1,2] indicate that this approximation holds to a relatively high degree of accuracy.

(3) Energy sharing and angular distributions[1,2] for the low excitation region of the residual nuclei are in rather good agreement with the momentum width of the expected deuteron-core wave function.

(4) Recent $(\pi^+,2p)$ experiments on ^{12}C and ^{32}S targets at 180 MeV which detect the γ rays resulting from excited states of the residual nucleus, show that the transitions to the 0^+, $T=1$ states in ^{10}B and ^{30}P are very weak[14] compared to transitions to unnatural parity states. These 0^+, $T=1$ states are known to have large parentage to the ground state of the target by coupling to a singlet deuteron.[15,16] Therefore, capture on an $S=0$, $T=1$ n-p pair is supressed, relative to capture on an $S=1$, $T=0$ n-p pair.

(5) Calculations by Schneider and Banerjee[17] based on a Fermi gas model for the nucleus indicate the dominance of capture on a n-p pair in a ^{3}S state. Finally, it is worth noting that even assuming capture on n-p pairs in other relative motion states is important; if the factorization approximation still holds, this two-body t matrix can be calculated independently.

Based on the above arguments we believe the present DWIA calculations of distortion effects should be generally applicable to the $(\pi,2N)$ reaction, and should provide guidance in the design and implementation of experiments. Unfortunately, as stated earlier, direct comparison of the calculations with currently available experimental data is almost impossible, due to the lack of sufficient energy resolution, the use of very large solid angles, and the absence of absolute cross section measurements, except as integrated over very specific experimental geometries.

In Sec. II, we briefly discuss the DWIA formulation and the ingredients in the present calculation. In Sec. III we present results, compared to plane

wave calculations, for the various angles, energies, and masses. Finally, in Sec. IV we discuss the implications and conclusions reached from these calculations.

II. DWIA FORMULATION

As stated in the Introduction, we assume that the $A(\pi^+,2p)B$ reaction proceeds via the capture of a pion on a neutron-proton cluster with the same relative motion and spin-isospin wave function as that of a physical deuteron. Following the DWIA cluster knockout formalism of Chant and Roos[18] we introduce the impulse approximation and replace the three-body t operator by the free two-body $\pi^+ + d \to 2p$ t operator. Furthermore, assuming that the resultant t matrix varies sufficiently slowly with momenta so that its arguments may be replaced by their asymptotic values, we obtain a factorized form for the transition amplitude. In particular, utilizing the notation of Ref. 18, the transition amplitude from an initial nuclear state with total angular momentum and isospin $J_A M_A, T_A N_A$ to a final nuclear state of B with quantum numbers $J_B M_B, T_B N_B$ is

$$T_{BA} = \left[\frac{A!}{B!2!}\right]^{1/2} \sum_{\alpha L J \sigma_b \Lambda M} \mathscr{I}_{AB}(\alpha L 1 J 0) \langle J M J_B M_B \mid J_A M_A \rangle \times \langle L \Lambda 1 \sigma_d \mid J M \rangle \langle \vec{k}_1, \vec{k}_2; \vec{\sigma}_1 \vec{\sigma}_2 \mid t_f^{(+)} \mid \vec{k}_\pi, \sigma_d \rangle \delta_{T_A T_B} \delta_{N_A N_B} \times \langle \eta_{B_{12}}^{(-)} \mid \delta(\vec{r}_\pi - \vec{r}_d) \mid \eta_{\pi A}^{(+)} \phi_{L\Lambda}^{\alpha}(\vec{r}_{dB}) \rangle \ . \tag{1}$$

In Eq. (1), $\mathscr{I}_{AB}(\alpha LSJT)$, the spectroscopic amplitude, and $\phi_{L\Lambda}^{\alpha}(\vec{r}_{dB})$, the center-of-mass wave function of the deuteron in the target nucleus, are related by

$$\langle \psi_{\substack{J_B M_B \\ T_A N_A}}(\tilde{B}) \psi_{\substack{1\sigma_d \\ 00}}(\tilde{d}) \mid \psi_{\substack{J_A M_A \\ T_A N_A}}(\tilde{A}) \rangle = \sum_{\alpha L J \sigma_b \Lambda M} \mathscr{I}_{AB}(\alpha L 1 J 0) \langle J M J_B M_B \mid J_A M_A \rangle \langle L \Lambda 1 \sigma_d \mid J M \rangle \phi_{L\Lambda}^{\alpha}(\vec{r}_{bB}) \ , \tag{2}$$

to the projection of the antisymmetrized target wave function $\psi(\tilde{A})$ onto a direct product of antisymmetrized deuteron and residual nucleus wave functions. It is assumed that isospin is conserved and α represents any additional quantum numbers required to specify the nuclear states. The vectors $\vec{k}_\pi$, $\vec{k}_1$, and $\vec{k}_2$ represent the asymptotic momenta of the incoming pion and outgoing protons. The wave functions $\eta_{\pi A}^{(+)}$ and $\eta_{B_{12}}^{(-)}$ describe the relative motion of the mass centers of the particles in the entrance and exit channels, respectively. Note that the use of a quasideuteron model limits us to transitions with $\Delta T = 0$, $\Delta S = 1$, and thus for 0^+ targets transitions to unnatural parity states.

Defining

$$S_{\alpha LJ}^{1/2} = \left[\frac{A!}{B!2!}\right]^{1/2} \mathscr{I}_{AB}(\alpha L 1 J 0) \ , \tag{3}$$

$$T_{BA}^{\alpha L \Lambda} = (2L+1)^{-1/2} \langle \eta_{B_{12}}^{(-)} \mid \delta(\vec{r}_\pi - \vec{r}_d) \mid \eta_{\pi A}^{(+)} \phi_{L\Lambda}^{\alpha}(\vec{r}_{dB}) \rangle \ , \tag{4}$$

the transition amplitude becomes

$$T_{BA} = \sum_{\alpha L J \Lambda M \sigma_b} S_{\alpha LJ}^{1/2} \langle J M J_B M_B \mid J_A M_A \rangle \langle L \Lambda 1 \sigma_d \mid J M \rangle (2L+1)^{1/2} T_{BA}^{\alpha L \Lambda} \langle \vec{k}_1 \vec{k}_2, \sigma_1 \sigma_2 \mid t_f^{(+)} \mid \vec{k}_\pi, \sigma_d \rangle \ . \tag{5}$$

The differential cross section, after averaging over M_A and summing over M_B, σ_1, and σ_2, becomes

$$\sigma_{BA} = \frac{2\pi}{\hbar v_\pi} W_B \sum_{\substack{\sigma_1 \sigma_2 \\ JM}} \frac{1}{(2J+1)} \left| \sum_{\alpha L \Lambda \sigma_d} S_{\alpha LJ}{}^{1/2} \langle L \Lambda 1 \sigma_d \mid J M \rangle (2L+1)^{1/2} T_{BA}^{\alpha L \Lambda} \langle \vec{k}_1 \vec{k}_2, \sigma_1 \sigma_2 \mid t_f^{(+)} \mid \vec{k}_\pi \sigma_d \rangle \right|^2 , \tag{6}$$

where v_π is the relative velocity of the π and target nucleus A and W_B is the energy density of final states.

In general, the summation over the orbital angular momentum transfer $L\Lambda$ is coherent even if the t matrix is independent of σ_d and spin-orbit distortions are excluded. However, assuming the $\pi^+ + d \to 2p$ t matrix is diagonal in the total spin projection (though not necessarily limited to a single channel spin) we may further simplify Eq. (6). This assumption should have little effect on our examination of distortion effects, and may be removed with a more detailed theory of the $\pi^+(NN)$ vertex. The resultant expression for the differential cross section is

$$\sigma_{BA} = \frac{2\pi}{\hbar v_\pi} W_B \, |\langle \bar{t} \rangle|^2 \sum_{LJ\Lambda} \left| \sum_\alpha S_{\alpha LJ}{}^{1/2} T_{BA}^{\alpha L\Lambda} \right|^2 , \tag{7}$$

where

$$|\langle \bar{t} \rangle|^2 = \sum_{\sigma_1\sigma_2\sigma_d} |\langle \vec{k}_1 \vec{k}_2, \sigma_1\sigma_2 | t_f^{(+)} | \vec{k}_\pi, \sigma_d \rangle|^2 . \tag{8}$$

In the special case of transitions in which only $L=0$ terms contribute, the form of Eq. (7) becomes exact without any assumptions as to the dependence of the t matrix on σ_d. If $T_{BA}^{\alpha L\Lambda}$ is independent of the additional quantum numbers α, we can define a spectroscopic factor

$$S_{LJ} = \left| \sum_\alpha S_{\alpha LJ}{}^{1/2} \right|^2 . \tag{9}$$

The evaluation of the amplitude $T_{BA}^{\alpha L\Lambda}$ requires the specification of the relative motion wave functions $\eta^{(\pm)}$ in the entrance and exit channels, as well as the deuteron cluster wave function. In the entrance channel we utilize a standard treatment of π-nucleus elastic scattering by a Kisslinger potential. In particular, $\eta_{\pi A}^{(+)}$ is the solution of the modified Klein-Gordon equation[19]

$$(-\nabla^2 + \mu^2)\eta = (E_\pi{}^2 - 2E_\pi V_c - U)\eta , \tag{10}$$

with

$$U\eta = -Ab_0 p_0{}^2 \rho\eta + Ab_1 \nabla(\rho\nabla\eta) . \tag{11}$$

For the exit channel scattering solution, we use the nonstatic approximation,[18,20] replacing the coupling term with its asymptotic value. This allows us to factorize the solution

$$\eta_{B_{12}}^{(-)} = \chi_{p_1B}^{(-)}(\vec{k}_{p_1B}, \vec{r}_{p_1B}) \chi_{p_2B}^{(-)}(\vec{k}_{p_2B}, \vec{r}_{p_2B}) , \tag{12}$$

where

$$(T_{p_1B} + V_{p_1B} - \epsilon_{p_1B}) \chi^{(-)}(\vec{k}_{p_1B}, \vec{r}_{p_1B}) = 0 , \tag{13}$$

$$(T_{p_2B} + V_{p_2B} - \epsilon_{p_2B}) \chi^{(-)}(\vec{k}_{p_2B}, \vec{r}_{p_2B}) = 0 . \tag{14}$$

The potentials V_{p_1B} and V_{p_2B} are taken to be optical potentials which describe proton-nucleus elastic scattering at the appropriate relative energies ϵ_{p_1B} and ϵ_{p_2B}. Details of this result and the kinematics are presented in Ref. 18.

Lastly, we need the wave function $\phi_{L\Lambda}^\alpha(\vec{r}_{dB})$, which results from the projection of the many-body wave function for A onto that of B and the deuteron. In the shell model this is, in principle, a straightforward calculation which has been used extensively in the analysis of two-nucleon transfer. However, for simplicity in the present calculations we have chosen to introduce a phenomenological Woods-Saxon potential $V_{\rm WS}$ which is adjusted to reproduce the empirical deuteron separation energy,

$$(T_{bB} + V_{\rm WS} - S_{Bd}) \phi_{L\Lambda}^\alpha(\vec{r}_{bB}) = 0 . \tag{15}$$

The quantum numbers for this wave function have been chosen on the basis of conservation of oscillator quanta with zero quanta in the deuteron cluster wave function. For single particles with quantum numbers $(n_1,l_1)(n_2,l_2)$ the c.m. quantum numbers of the deuteron cluster (N,L) are

$$2(n_1-1) + l_1 + 2(n_2-1) + l_2 = 2(N-1) + L . \tag{16}$$

This procedure has been shown to reproduce the shape of a more correct calculation rather well.

To summarize, the cross section expression for a specific L,J transfer including fully relativistic expressions for the phase space and incident flux becomes

$$\frac{d^3\sigma^{LJ}}{d\Omega_1 d\Omega_2 dE_1} = |\langle \bar{t} \rangle|^2 S_{LJ} \left\{ \frac{E_\pi E_1 E_2}{(2\pi)^5 (\hbar c)^7} \frac{P_1 P_2 c}{P_\pi} \frac{1}{1 + (E_2/E_B)[1 - (P_\pi/P_2)\hat{k}_\pi \cdot \hat{k}_2 + (P_1/P_2)\hat{k}_1 \cdot \hat{k}_2]} \right\} \sum_\Lambda |T_{BA}^{\alpha L\Lambda}|^2 , \tag{17}$$

where

$$T_{BA}^{\alpha L\Lambda}=\frac{1}{(2L+1)^{1/2}}\int \chi_{p_1B}^{(-)*}(\vec{k}_{p_1B},\vec{r})\chi_{p_2B}^{(-)}(\vec{k}_{p_2B},\vec{r})\chi_{\pi A}^{(+)}(\vec{k}_{\pi A},\gamma\vec{r})\phi_{L\Lambda}^{\alpha}(\vec{r})d^3r\ , \tag{18}$$

$\gamma=B/A$, $\chi_{\pi A}^{(+)}=\eta_{\pi A}^{(+)}$, and E_i is the total energy for particle i. For convenience and use in later sections we can replace the $|\langle\hat{t}\rangle|^2$ by the two-body cross section and rewrite Eq. (17) in the form

$$\frac{d^3\sigma^{LJ}}{d\Omega_1 d\Omega_2 dE_1}=KS_{LJ}\cdot\frac{d\sigma}{d\Omega}\bigg|_{\pi^++d\to 2p}\sum_{\Lambda}|T_{BA}^{\alpha L\Lambda}|^2\ , \tag{19}$$

where K contains the kinematic factors present in Eq. (17) as well as those required to replace $|\langle\hat{t}\rangle|^2$ by $d\sigma/d\Omega$.

In the limit of no distortions the above expressions reduce to the plane wave impulse approximation (PWIA). Specifically, the distorted waves χ in Eq. (18) reduce to plane waves and the quantity $T_{BA}^{\alpha L\Lambda}$ is proportional to the Fourier transform of the deuteron cluster c.m. wave function. For this reason $|T_{BA}^{\alpha L\Lambda}|^2$ is often referred to as the distorted momentum distribution. An expression equivalent to the plane wave limit of Eq. (19) was used by both Favier *et al.*[1] and Arthur *et al.*[2] in the analysis of their $(\pi^+,2p)$ data.

The DWIA cross sections to be described were evaluated using a version of the DWIA cluster knockout code THREEDEE, modified to include pion elastic scattering wave functions. The code performs a direct integration in (r,θ,ϕ) leading to a large increase in speed over conventional partial wave decompositions.

Before proceeding to the next section it is worthwhile to recall that our major approximation (in addition to the use of a distorted wave theory) is probably the restriction of the calculation to capture on quasideuterons. The decomposition of almost any A-body wave function into $B+(np)$ shows the existence of a number of terms with relative motion different from that of the ^3S state of a deuteron. However, as our understanding of the π capture process grows one will be able to evaluate the importance of other configurations. Furthermore, if the factorized impulse approximation we have used proves satisfactory, a result which can be tested experimentally, our approach can be generalized to include other elementary $\pi(2N)$ amplitudes and to take proper account of the omitted coherence between different amplitudes.

III. DWIA CALCULATIONS

To carry out these calculations the pion optical model code DUMIT[21] was combined with the DWIA code THREEDEE. Since our interest was to study distortion effects systematically over a range of mass and energy, we wanted to use systematic optical model potentials. For the pion channel we chose to use phenomenological choices of the s- and p-wave parameters b_0 and b_1. For bombarding energies in excess of $T_\pi=100$ MeV we have utilized the recent results of Cottingame and Holtkamp,[22] who obtain reasonable fits to the experimental data in the resonance region by using the free π-N parameters from an energy approximately 30 MeV lower than that of the bombarding energy. For lower energies, $T_\pi<100$ MeV, we have combined the work of Dytman *et al.*[23] and Amann *et al.*[24] Dytman *et al.* show that at 50 MeV an average set of b_0 and b_1 provide acceptable fits to nuclei from ^{12}C to ^{54}Fe. From fits to ^{12}C data from 28 to 88 MeV, Amann *et al.*[24] obtain a linear energy dependence for the b's. We therefore use the expressions of Amann *et al.* and assume that these parameters provide equivalent fits to all nuclei with $N\simeq Z$. We believe that this potential is sufficient to obtain a good understanding of the distortion effects particularly in the lower energy region where the pion absorption is not strong.

For the proton optical potentials we have used the results of Nadasen *et al.*[25] The global potential presented in that work was obtained from an analysis of nuclei ranging from ^{28}Si to ^{208}Pb over an energy range of about 40 to 180 MeV. Again, we believe this potential to be sufficient, even for the light elements, to provide a global understanding of distortion effects in the $(\pi^+,2p)$ reaction.

Finally, the Woods-Saxon potential for the bound deuteron cluster wave function was assumed to have a geometry of $r_0=1.3$ fm, $a=0.65$ fm, which yields wave functions having rms radii close to the rms radii of the various target nuclei.

Although many of the results presented exclude the two-body $\pi^++d\to 2p$ cross section, in those cases where it is used we have approximated it by the on-shell cross section corresponding to the final state of the two protons (final energy prescription). In principle, of course, the struck deuteron is of order 20 MeV off the mass shell.

As a first examination of distortion effects we have calculated the $(\pi^+,2p)$ cross sections for $L=0$ transitions to low-lying states in the residual nucleus over an incident pion energy range of 25 to 350 MeV. In Fig. 1(a) we present the results for the coplanar symmetric case with $\theta_1=-\theta_2$, $E_1=E_2$, and zero recoil momentum for the residual nucleus. To clearly identify the specific effects of distortion we have plotted the ratio of the distorted wave to the plane wave cross section.

This graph shows a number of features. Firstly, there is an obvious discontinuity near 100 MeV, where our choice of pion potentials change. This is not unexpected since this bombarding energy is on the high side of the analysis of Amann *et al.*[24] and the low side of the analysis of Cottingame and Holtkamp.[22] One should probably ignore the details of the calculation over the energy range of 80 to 120 MeV due to these inconsistencies. Secondly, as expected, the absorption reflects the π-nucleon (3,3) resonance and is strongest near the resonance.

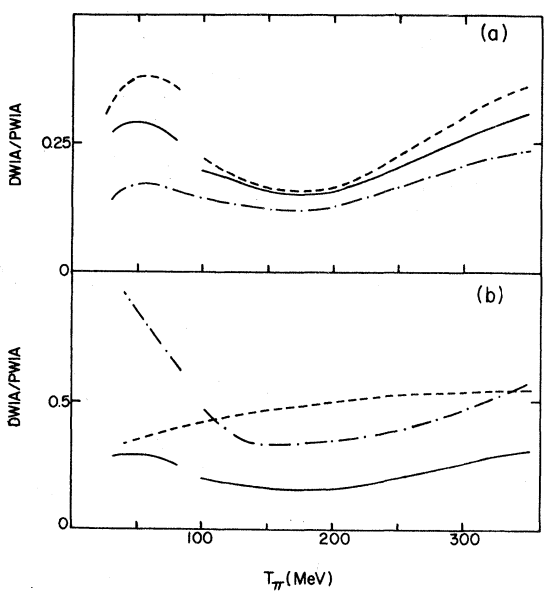

FIG. 1. Ratio of distorted wave to plane wave cross sections for the $(\pi^+,2p)$ reaction as a function of the pion bombarding energy. The cross sections were calculated for a co-planar symmetric geometry with $\theta_1=-\theta_2$, $E_1=E_2$, $L=0$, and zero recoil momentum for the residual nucleus; (a) target nuclei ^{16}O (— — —), ^{40}Ca (——), and ^{90}Zr (-·-); (b) ratios for ^{40}Ca with plane waves in the π^+ channel (— — —), plane waves in the proton channels (-·-), and the full distorted wave calculation (——).

The differences in absorption between the three nuclei is least on the resonance. Thirdly, even on the resonance the reduction is not very large, being comparable to similar calculations for $(p,2p)$ in the 200 to 400 MeV range,[26] and significantly smaller than $(p,p\alpha)$ in the same energy range.[27] Thus, one expects distorted wave treatments of the interaction with the residual core to be adequate. Finally, these results are similar in shape to poor resolution studies of the $(\pi^+,2p)$ reaction over a comparable energy range. For example, Bressani *et al.*[28] plot the ratio of the $A(\pi^+,2p)$ cross section to the $(\pi^+ + d \rightarrow 2p)$ cross section for several light nuclei as a function of bombarding energy. These data show a small dip in this ratio near the resonance.

In order to examine the origin of the shape of the curves in Fig. 1(a) in more detail, we have carried out a series of calculations for ^{40}Ca$(\pi^+,2p)$ with either the π^+ or the two proton distortions omitted, i.e., plane waves either in the entrance or exit channels. These results are plotted in Fig. 1(b). The curve with no proton distortion clearly shows the strong effect of the (3,3) resonance with reduced absorption on either side. The effect of proton distortion, on the other hand, falls monotonically as the proton energy increases. It is interesting to note that the product of the two ratio calculations (no π^+ distortion and no proton distortion) is very nearly equal to the result of the full calculation. This suggests that the calculations for this geometry involve no strong interference effects, but rather a simple attenuation of the plane waves.

Finally, to show explicitly the dependence of the $(\pi^+,2p)$ cross section for zero recoil momentum with symmetric geometry, we have plotted the ^{40}Ca

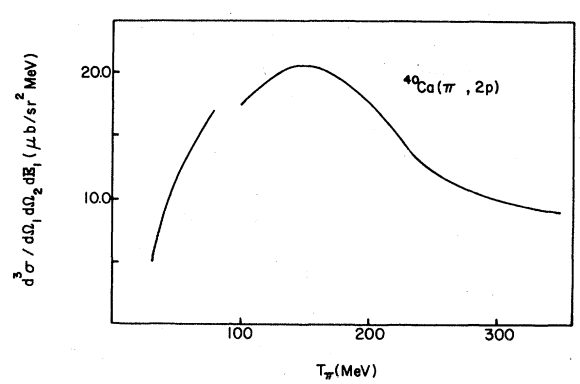

FIG. 2. The DWIA cross section for ^{40}Ca$(\pi^+,2p)^{38}$K as a function of bombarding energy. See caption for Fig. 1.

results multiplied by the 90° $\pi^+ + d \rightarrow 2p$ two-body cross section.[29] This result, assuming a spectroscopic factor of unity, is plotted in Fig. 2. Although the attenuation is largest in the resonance region, the shape of the cross section is dominated by the two-body $\pi^+ + d \rightarrow 2p$ cross section showing the resonance behavior. It is interesting to note that this shape is almost identical to that measured for the energy dependence of the pion absorption cross section.[30]

B. Energy sharing distributions

One of the most common measurements made in three-body final state reactions is to determine an energy sharing distribution, i.e., $d^3\sigma/d\Omega_1 d\Omega_2 dE_1$, the cross section for the population of a particular final state in the residual nucleus as a function of the energy of one of the outgoing particles. In the PWIA limit of our quasideuteron model, this cross section is proportional to the square of the deuteron cluster-core momentum wave function in the target nucleus.

We have carried out calculations of $L=0$ transitions for ^{16}O and ^{90}Zr and $L=0$ and $L=2$ transitions for ^{40}Ca, again with a co-planar symmetric geometry allowing zero recoil momentum for the residual nucleus. Again, to show the energy dependence of the distortion effects, we have plotted the distorted momentum distribution $\sum_\Lambda | T_{BA}^{\alpha L \Lambda} |^2$ [see Eq. (19)] as a function of recoil momentum for three pion bombarding energies below, on, and above the resonance. These results are shown in Figs. 3–5, along with a plane wave momentum distribution for comparison. The absolute cross sections at zero recoil momentum for these calculations, assuming $C^2S=1$, can be obtained from Fig. 2.

From Figs. 3–5 we see that at all three energies the distorted momentum distribution reflects the true momentum distribution of the deuteron cluster relatively well. For the $L=0$ transitions minima in the distorted momentum distribution arise from the nodes in the deuteron cluster wave functions, $2S$ for ^{16}O, $3S$ for ^{40}Ca, and $4S$ for ^{90}Zr. Although the distortion effects at zero recoil momentum are largest at 180 MeV, the effect is primarily that of absorption (attenuation), thereby generally preserving the shape of the momentum distribution. As a result the 40 MeV calculation least accurately reflects the momentum distribution, and the distortion effects fill in and shift the minima. Similarly, for the $L=2$ calculations (Fig. 4), the minimum at

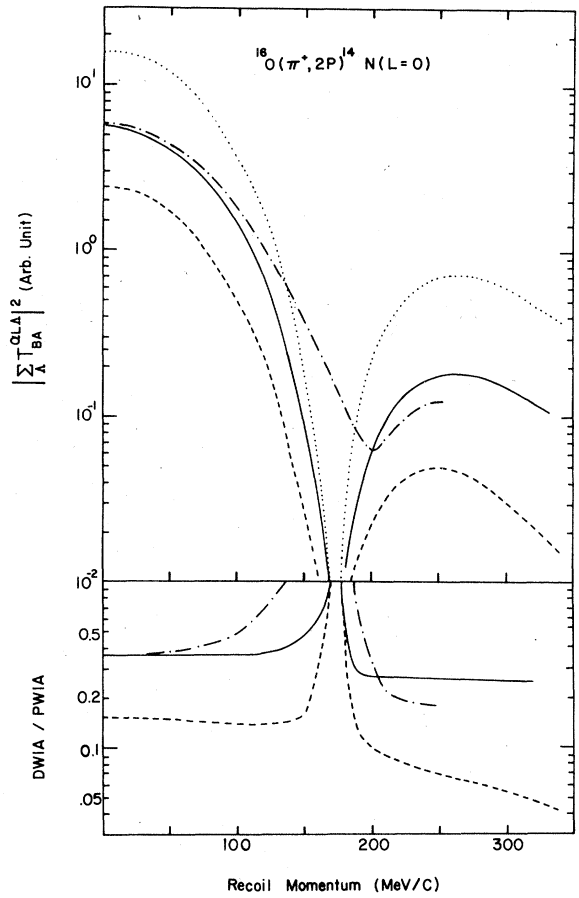

FIG. 3. Calculated distorted momentum distributions for ^{16}O(π^+,2p)^{14}N ($L=0$, $Q=117.1$ MeV) at three bombarding energies as a function of the recoil momentum of the residual nucleus. The calculations represent an energy sharing distribution for a co-planar symmetric geometry: $T_\pi=40$ MeV, $\theta_1=-\theta_2=81.7°$(···); $T_\pi=180$ MeV, $\theta_1=-\theta_2=74.8°$ (— — —); $T_\pi=350$ MeV, $\theta_1=-\theta_2=70.5°$ (——); plane waves (· · ·).

zero recoil momentum is greatly modified, and at 40 MeV it actually becomes a small maximum for ^{40}Ca. Note also that the peak of the $L=2$ distribution is at least of factor of 10 smaller than that of the $L=0$ distribution. Thus, experimental geometries emphasizing recoil momenta near zero will predominantly select the $L=0$ transitions.

The modification of the momentum distribution by distortion effects is more graphically illustrated by the bottom panels in Figs. 3–5. Here we have plotted the ratio of the distorted wave to plane wave momentum distribution for each point on the energy sharing distribution. These curves show the

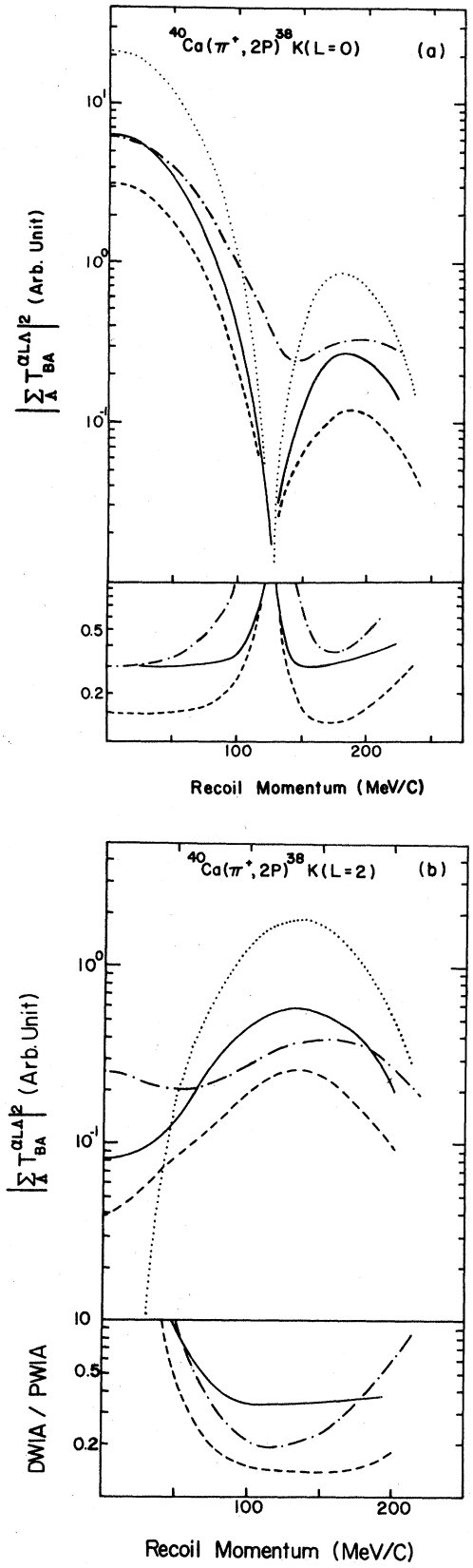

FIG. 4. (a) Calculated distorted momentum distributions for the ^{40}Ca(π^+,2p)^{38}K ($L=0$, $Q=118.1$ MeV) at three bombarding energies as a function of the recoil momentum of the residual nucleus. The calculations represent an energy sharing distribution for a co-planar symmetric geometry: $T_\pi=40$ MeV, $\theta_1=-\theta_2=81.7°$ (-·-); $T_\pi=180$ MeV, $\theta_1=-\theta_2=74.8°$ (— — —); $T_\pi=350$ MeV, $\theta_1=-\theta_2=70.5°$ (——); plane waves (· · ·). (b) Same as (a), but with orbital angular momentum $L=2$.

pronounced effect of distortion around the minima, but also show that near the peaks of the distribution the distortion effect is relatively constant.

Overall, the calculations suggest that the distortion effects do not greatly modify the momentum distribution measured in an energy sharing experiment. Furthermore, even at the relatively low energy of 40 MeV, a region in which the experiment may be performed more easily, the resultant data should provide reasonable details of the cluster wave function, assuming, of course, the applicability of our quasideuteron model.

Finally, to relate these present calculations of the energy sharing distributions more closely to experiment, we have plotted the calculated ^{40}Ca(π^+,2p) cross sections, using $C^2S=1$ and the final energy prescription, versus the energy of one of the outgoing protons. These results are displayed in Fig. 6. As can be seen, the cross sections are relatively small, explaining in large part the challenge in obtaining significant amounts of quality data.

C. Radial localization

An alternative method of examing distortion effects, used quite successfully for the understanding of alpha-cluster knockout reactions,[18,31] is to calculate the cross section contributions as a function of radius. We have calculated the (π^+,2p) cross section for a series of lower radial cutoffs in the distorted wave integral of Eq. (18). The resultant cross sections are then differenced for adjacent cutoff radii and the difference $\Delta\sigma$ is plotted as a function of radius; i.e., $\Delta\sigma(r)=\sigma(r+\Delta)-\sigma(r)$, where $\sigma(x)$ is the cross section calculated with the radial cutoff x. Such a procedure provides a simple means of understanding the sensitivity of the reaction to various radial regions, and thereby the degree of radial localization of a given reaction.

The most transparent case for examination of $\Delta\sigma$ is that of the zero recoil momentum point for an $L=0$ transition. Note that for plane waves

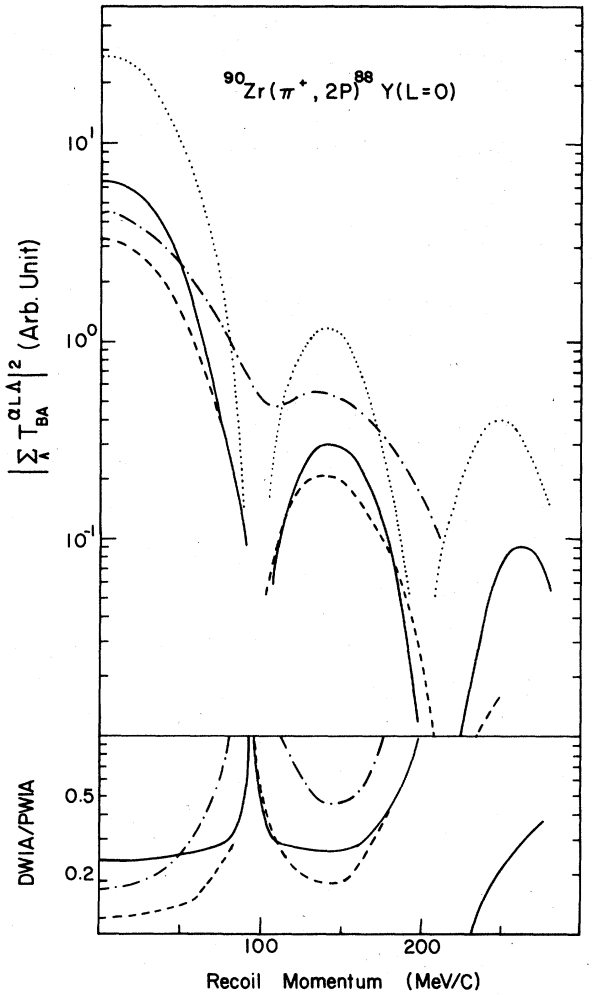

FIG. 5. Calculated distorted momentum distributions for the ^{90}Zr(π^+,2p)^{88}Y ($L=0$, $Q=119.8$ MeV) at three bombarding energies as a function of the recoil momentum of the residual nucleus. The calculations represent an energy sharing distribution for a co-planar symmetric geometry: $T_\pi=40$ MeV, $\theta_1=-\theta_2=81.8°$ (— · —); $T_\pi=180$ MeV, $\theta_1=-\theta_2=74.9°$ (— — —); $T_\pi=350$ MeV, $\theta_1=-\theta_2=70.5°$ (——); plane waves (· · ·).

(PWIA) this case corresponds to an integrand which is equal to the bound cluster wave function. The resultant $\Delta\sigma$ for $L=0$ (π^+,2p) transitions on ^{16}O, ^{40}Ca, and ^{90}Zr are shown in Fig. 7. Calculations are presented for 40, 180, and 350 MeV, along with plane wave calculations for comparison. From these calculations we can now understand much of the behavior presented in the previous two sections. In particular, the primary effect of the distorted waves is to gradually attenuate the contributions of the bound cluster wave function as the

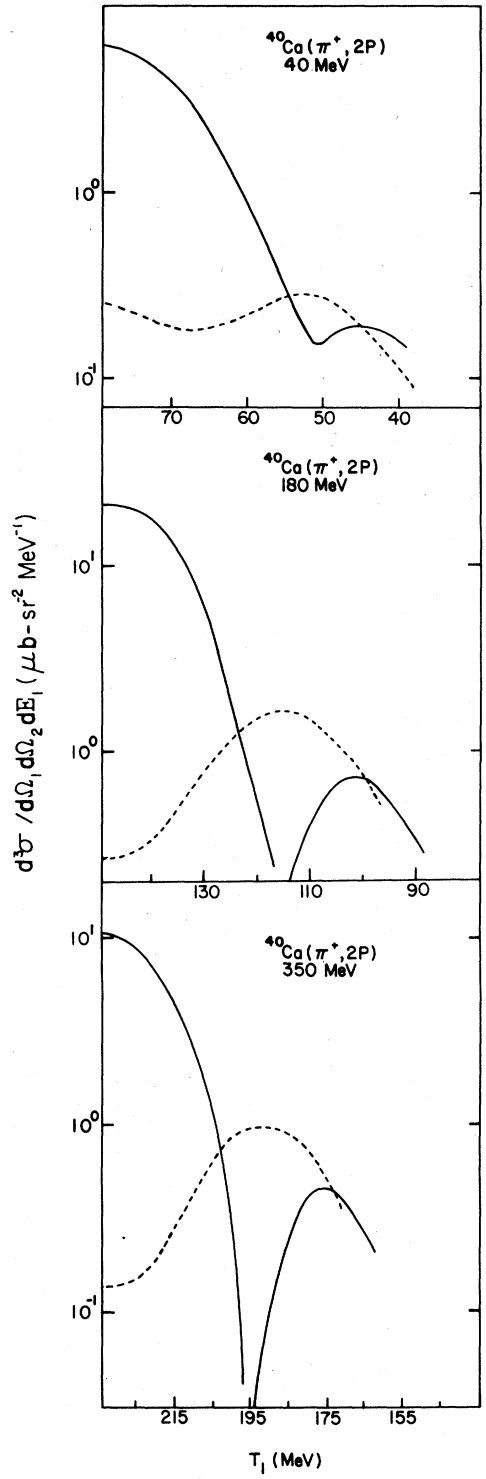

FIG. 6. DWIA energy sharing cross sections for the ^{40}Ca(π^+,2p)^{38}K reaction as a function of the energy of one of the outgoing protons. The calculations are the same as presented in Figs. 4(a) and (b); $L=0$ (——) and $L=2$ (— — —).

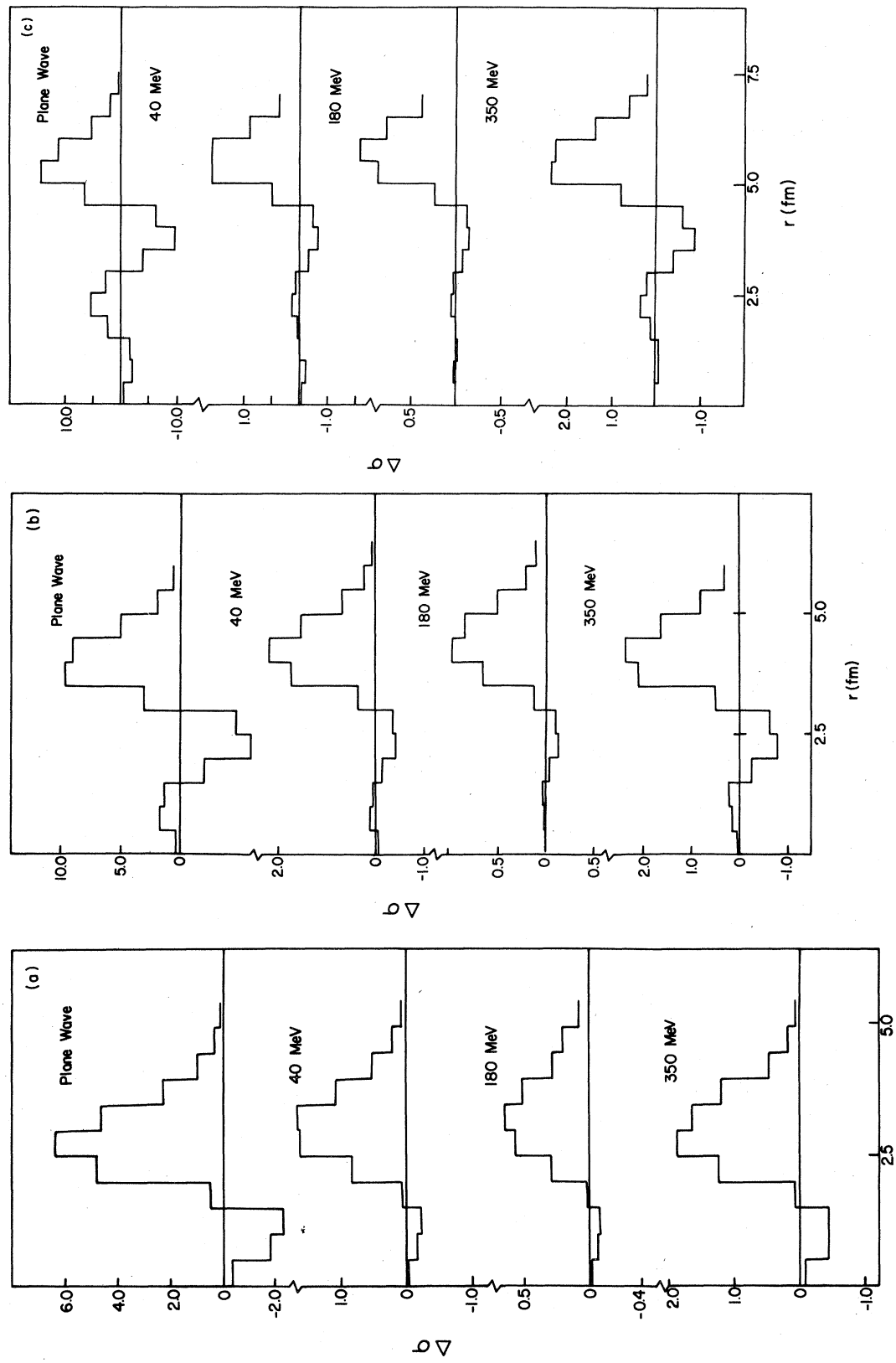

FIG. 7. (a) Change in $^{16}O(\pi^+,2p)^{14}N$ DWIA cross section $\Delta\sigma$ with cutoff radius as a function of radius. The results are for the $L=0$, zero recoil momentum points presented in Fig. 3. (b) $\Delta\sigma$ for $^{40}Ca(\pi^+,2p)^{38}K$ for the $L=0$, zero recoil momentum point of Fig. 4(a). (c) $\Delta\sigma$ for $^{90}Zr(\pi^+,2p)^{88}Y$ for the $L=0$, zero recoil momentum point of Fig. 5.

radius decreases. Thus, the real optical potentials which can change the phasing in the nuclear interior are not playing a major role. Unlike $(p,p\alpha)$ or $(\alpha,2\alpha)$ reactions[18,31] which are strongly surface localized, the $(\pi^+,2p)$ reaction is sensitive to the full radial extent of the nucleus. These calculations thus explain why the structure of the momentum distribution is generally preserved in the DWIA calculations for the energy sharing distributions. One also observes the other expected features, namely, that the attentuation increases with increasing mass and that the attentuation is more pronounced at 180 MeV than at 40 or 350 MeV.

IV. CONCLUSIONS

The present DWIA calculations show that it is essential to include distortion effects arising from the residual core in any quantitative comparison with $(\pi^+,2p)$ data. Neglect of these distortions can lead to errors of as much as a factor of 7 in the calculated cross section, and thereby the spectroscopic information. However, the present calculations show several very encouraging features. Firstly, these distortions are sufficiently small that a distorted wave treatment of them should be fully adequate. Secondly, the $(\pi^+,2p)$ reaction in fact samples essentially the full radial extent of the nucleus, and is therefore one of the few reactions to do so. Thirdly, the distortion effects are very similar over the full energy range studied in this paper. Thus, assuming the applicability of the present calculations, experiments at lower energy, where the proton detection is more easily performed, provide as much information as those at higher energy. Finally, the energy sharing distributions contain rather directly the information on the momentum distribution of deuteron clusters in nuclei.

We believe the present calculations enhance our understanding of the $(\pi^+,2p)$ reaction mechanism. With the acquisition of high quality $(\pi^+,2p)$ data to discrete states, one can begin to understand the validity of the present quasideuteron DWIA calculation. If the validity of the approximation can be demonstrated, one can then begin detailed comparisons to examine whether the reaction is dominated by longer ranged correlations, such as those contained in standard shell model calculations, or whether the data contain any evidence for short-ranged correlations. If, on the other hand, precise data for discrete states show the quasideuteron approach to be inadequate, the present calculations can be modified in a factorized form to include a more detailed treatment of the $\pi(NN)$ vertex. Independent of the result, we have demonstrated the importance of including interactions with the core nucleus, and believe the general effects shown will persist for any likely reaction mechanism.

ACKNOWLEDGMENTS

We are indebted to E. Rost for providing a copy of the code DUMIT and for assistance with minor modifications thereto. We thank Karen Stricker for a clue to deciphering some of the more cryptographic literature on pion elastic scattering. Finally, we thank the University of Maryland Computer Science Center for generous provision of UNIVAC 1108 computer time. This work was supported in part by a grant from the U.S. National Science Foundation.

[1]J. Favier *et al.*, Nucl. Phys. A169, 540 (1971).
[2]E. D. Arthur *et al.*, Phys. Rev. C 11, 332 (1975).
[3]B. Bessalleck *et al.*, Phys. Rev. C 19, 1893 (1979).
[4]H. Ullrich, *Meson-Nuclear Physics—1979 (Houston)*, Proceedings of the 2nd International Topical Conference on Meson-Nuclear Physics, edited by E. V. Hungerford III (AIP, New York, 1979), p. 154.
[5]J. Niskanen, Nucl. Phys. A298, 417 (1978).
[6]J. Chai and D. O. Riska, Nucl. Phys. A338, 349 (1980).
[7]D. S. Koltun and A. Reitan, Nucl. Phys. B4, 629 (1968).
[8]D. S. Koltun, Adv. Nucl. Phys. 3, 71 (1969).
[9]T. I. Kopaleishvili, Part. Nucl. 22, 87 (1973).
[10]F. Hachenberg, J. Hufner, and H. J. Pirner, Phys. Lett. 66B, 425 (1977).
[11]R. S. Bhalerao and Y. R. Waghmare, Nucl. Phys. A298, 367 (1978).
[12]H. Garriliazo and J. M. Eisenberg, Nucl. Phys. A220, 13 (1974).
[13]K. Shimizu and Amand Faessler, Nucl. Phys. A306, 311 (1978); Phys. Rev. C 19, 1891 (1978).
[14]C. E. Stronach *et al.*, Phys. Rev. C 23, 2150 (1981).
[15]For example, see the $^{12}C(p,^3He)^{10}B$ results of C. G. Hoot, D. K. Olsen, R. E. Brown, J. R. Maxwell, and A. Scott, Nucl. Phys. A203, 339 (1973).
[16]For example, see the $2s$-$1d$ shell model wave functions of B. H. Wildenthal, J. B. McGrory, E. C. Halbert,

and H. D. Graber, Phys. Rev. C 4, 1703 (1971).
[17]D. Schneider and M. Banerjee (private communication).
[18]N. S. Chant and P. G. Roos, Phys. Rev. C 15, 57 (1977).
[19]E. H. Auerbach, D. M. Fleming, and M. M. Sternheim, Phys. Rev. 162, 1683 (1967).
[20]R. D. Koshel, Nucl. Phys. A260, 401 (1976).
[21]E. Rost (private communication).
[22]W. B. Cottingame and D. B. Holtkamp, Phys. Rev. Lett. 45, 1828 (1980).
[23]S. A. Dytman *et al.*, Phys. Rev. C 19, 971 (1979).
[24]J. F. Amann *et al.*, Phys. Rev. C 23, 1635 (1981).
[25]A. Nadasen *et al.*, Phys. Rev. C 23, 1023 (1981).
[26]P. G. Roos, *Momentum Wave Functions—1976 (Indiana University)*, Proceedings of the Workshop/Seminar on Momentum Wave Function Determination in Atomic, Molecular, and Nuclear Systems, edited by D. W. Devins (AIP, New York, 1977), p. 32.
[27]N. S. Chant, *Clustering Aspects of Nuclear Structure and Nuclear Reactions (Winnipeg, 1978)*, Proceedings of the Third International Conference on Clustering Aspects of Nuclear Structure and Nuclear Reactions, edited by W. T. H. Van Oers *et al.* (AIP, New York, 1978).
[28]T. Bressani *et al.*, Nucl. Phys. B9, 427 (1969).
[29]The 90° cross section was approximated by drawing smooth curves through a subset of experimental values present graphically in Ref. 5.
[30]D. Ashery *et al.*, Phys. Rev. C 23, 2173 (1981).
[31]C. W. Wang, N. S. Chant, P. G. Roos, A. Nadasen, and T. A. Carey, Phys. Rev. C 21, 1705 (1980).